TR–92–007

Kinematic Identification of an Active Binocular System Using Stereo Vision

Sheng–Wen Shih, Jia–Sheng Jin, Kuo–Hua Wei,
Yi–Ping Hung

Insititute of Information Science
Academia Sinica
NanKang, Taipei, Taiwan, 115
Republic of China

TR–92–007

Kinematic Identification of an Active Binocular System Using Stereo Vision

Sheng–Wen Shih, Jia–Sheng Jin, Kuo–Hua Wei,
Yi–Ping Hung

Insititute of Information Science
Academia Sinica
NanKang, Taipei, Taiwan, 115
Republic of China

Kinematic Identification of an Active Binocular System Using Stereo Vision

Sheng-Wen Shih[1][3], Jia-Sheng Jin[1][2], Kuo-Hua Wei[1], Yi-Ping Hung[1]

[1]Institute of Information Science, Academia Sinica.
[2]Institute of Computer Science and Information Engineering, National Taiwan University.
[3]Institute of Electrical Engineering, National Taiwan University.

ABSTRACT

This paper describes the process of calibrating the kinematic model for an active binocular head having four revolute joints and two prismatic joints. We use the complete and parametrically continues (CPC) model proposed by Zhuang and Roth in 1990 to model the motorized head, and use a closed form solution to identify its CPC kinematic parameters. The calibration procedure is divided into two stages. In the first stage, the two cameras are replaced by two calibration plates each having nine circles. The two removed cameras can be used to build a stereo vision system for observing the varying positions and orientations of the calibration plates when moving the joints of the head. The positions and orientations of the calibration plates, or equivalently, of the end-effectors, can be determined from the stereo measurements. The acquired data are then used to calibrate the kinematic parameters. In the second stage, the cameras are remounted to the IIS-head, and a method proposed by Tsai is used to calibrate the hand-eye relation. Once the above kinematics calibration is done, we shall be able to control the binocular head to gaze or track 3D targets.

1. INTRODUCTION

Recently a significant amount of work in computer vision has focused on the problems of acting, behaving systems, and in particular on how "active vision" differs from vision with fixed cameras.

In an active stereo system, the cameras are able to preform functions such as gazing, panning and tilting. As shown in Fig. 1., we have designed and implemented an active vision system, called the IIS–head, which has four revolute joints and two prismatic joints. The two joints on top of the IIS–head are for camera vergence or gazing (referred to as joint 5^L and joint 5^R). The next two joints below them are for tilting and panning the stereo cameras (referred to as joint 4 and joint 3). All of the above four joints are revolute, and are mounted on an X–Y table which is composed of two prismatic joints (referred to as joint 2 and joint 1). Since the IIS–head is built with off–the–shelf components, its kinematic parameters are unknown. Our goal is to calibrate its kinematic parameters for controlling the orientations and positions of the stereo cameras.

According to the scheme of Roth, Mooring, and Ravani[15], robot calibration may be divided into three levels. Level 1 is defined as "Joint Level Calibration". At this level, the primary goal is to determine the correct relationship between the joint transducer signal and the actual joint displacement. Level 2 is defined as "Kinematic Model Calibration". At Level 2, the goal is to improve the accuracy of the kinematic model of the manipulator. With this type of calibration, the assumption is usually made that the links of the manipulator are rigid and the joints are either revolute or prismatic. Level 3 is "Nongeometric Calibration". At this level the effects due to backlash, eccentricity in the

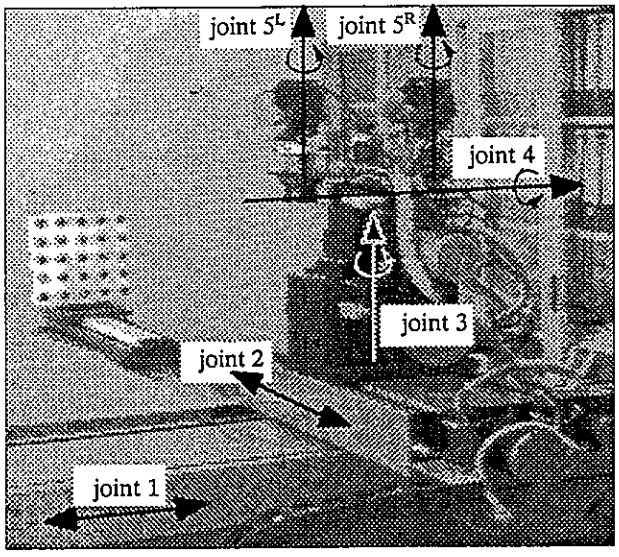

Fig. 1. A picture of the IIS–head

joint gearing, joint compliance, link compliance, friction and dynamic model are calibrated. In this paper, we will focus on the first two levels of calibration.

In general, calibration process consists of four major steps[9]. The first step would be to choose the form of a suitable functional relationship, i.e., the kinematic modeling step. The second step would be to collect measurement data needed for accurate kinematic identification of the robot, i.e., the data collection step. The third step would be the computational process of using the data collected to identify the parameters in the model, i.e., the identification step. The final step would be the implementation of the new model in the position control software for the robot, i.e., the correction step. The correction step is not presented here, since in practice, the implementation of the new model is quite straight forward.

Section 2 explains why we adopt CPC model, rather than the D–H model or the S–model, for the kinematic of the IIS–head, and then gives a brief review of the CPC model. Data collection using stereo vision is described in section 3. Section 4 shows the details of the closed form solution for identifying the kinematic parameters of the IIS–head. Section 5 mentions the second stage of the calibration: hand–eye calibration. Section 6 shows some experimental results and section 7 gives some concluding remarks.

2. KINEMATIC MODELING FOR THE IIS–HEAD

The most popular kinematic model for a manipulator is the Denavit–Hartenberg (D–H) model[4]. But there are several problems associated with the use of the D–H model. First, most calibration methods based on D–H model are actually processes of improving the accuracy of the existing model, while the nominal model is not readily available for the IIS–head we built. Second, D–H model does not determine the correct relationship between the joint transducer signal and the actual joint displacement, i.e., one further procedure is needed to complete the joint level calibration. We prefer a model having the zero position of the joint variables correspond to the zero reading of the joint transducers. Third, D–H model is not complete for the IIS–head. The hand/eye transformation should have six degrees of freedoms, while the four parameters of the D–H model are not enough for expressing it. Forth, D–H model is not parametrically continuous, in general. When two consecutive joint axes are parallel, there are infinite number of common normals of the same length, hence the location of the axis coordinate system may be made arbitrarily. But if these axes are slightly misaligned and intersect with each other, i.e., they are coplanar, the length of the common normal reduces

to zero abruptly. Also, the location of the axis coordinate system jumps far away along the joint axis. To deal with this discontinuity, many people treat two consecutive parallel joints as an exception and use a modified formulation to determine the joint–to–joint transformation matrix.

One possible model for solving this discontinuity problem is the S–model[18]. Because each link transformation matrix is specified by six parameters rather than by four, the S–model convention is less restrictive than the D–H model convention. In S–model the origin of frame *i–1* is not forced to lie at the intersection point of the joint *i* axis and the common normal between the joint *i–1* and joint *i* axis. The location of the origin of frame *i–1* on the joint *i* axis is arbitrary since the S–model has an offset parameter. Another advantage of the S–model convention is that the direction of the x axis of frame *i–1* only have to be orthogonal to the z axis of frame *i–1* because of introducing a new parameter. These two added parameters provide the arbitrary location of origin of the frame along the joint axis and the arbitrary orientation of the x axis of the frame so that the S–model is complete. More importantly, the degree of freedom of being able to assign frame origin on joint axis may avoid the disadvantage of not being parametrically continuous, because it can compensate the distance when the frames' origins in the D–H model jump far away. Although the S–model is complete and parametrically continuous, we choose to use the CPC model[23] because it has closed–form solutions[24] and does not require nominal model.

2.1 A Singularity–Free Line Representation

Robert[14] indicated that the lack of parametrically continuity of the D–H model is due to the singularity of D–H line representation, i.e., the way they represent one joint axis (a straight line) in another joint frame is singular in some configurations. He then proposed a new representation for a line in Euclidean *n*–space, say $n = 3$, which uses only $2n-2 = 4$ parameters (the minimum number possible). Unlike other 4–parameter representations, it has no singularities and special cases.

2.2 CPC Model

Based on Roberts' singularity–free line representation, Zhuang and Roth proposed the CPC model for robot manipulators[23]. Consider a robot with n joints which can be either *ideally revolute* or *ideally prismatic*. Let $\{x_i, y_i, z_i\}$ be the frame *i* coordinate system associated with the joint $i+1$, $\{x_0, y_0, z_0\}$ be the base coordinate system, and $\{x_n, y_n, z_n\}$ be the end–effector coordinate system. Let ${}^{i}\mathbf{T}_{j}$ be the 4×4 homogeneous transformation matrix from the frame *i* coordinate system to the frame *j*

coordinate system, and ${}^{w}\mathbf{T}_n$ be the 4×4 homogeneous transformation matrix from the world coordinate system (WCS) to the end–effector coordinate system. Then we have

$$ {}^{w}\mathbf{T}_n = {}^{w}\mathbf{T}_0 {}^{0}\mathbf{T}_1 \cdots {}^{n-2}\mathbf{T}_{n-1} {}^{n-1}\mathbf{T}_n . \tag{1} $$

In general, the positions and orientations of the world coordinate system (frame w) and the end–effector coordinate system (frame n) can be assigned arbitrarily. All other link frames (frame *0, 1, ..., n–1*) are established based on the following convention:

1. The z_i–axis is assigned to be parallel to the $i+1$st joint axis.
2. The coordinate frame $\{x_i, y_i, z_i\}$ forms an orthonormal right–hand system.

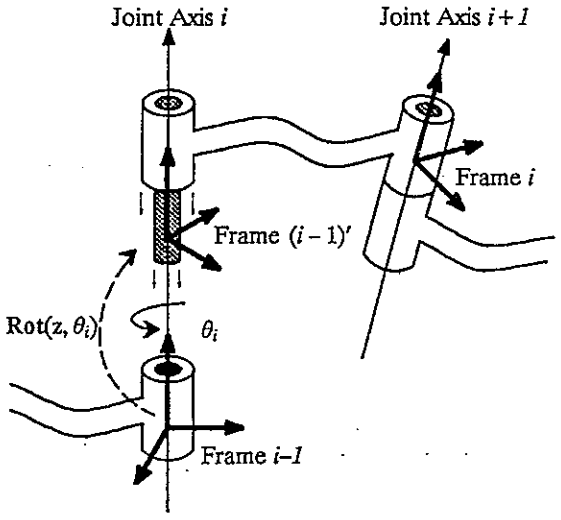

Fig. 2. CPC modeling convention for a revolute joint

For convenience, let $\mathbf{Rot}(\hat{\mathbf{k}}, \alpha)$ denote the homogeneous rotation matrix rotating about the axis $\hat{\mathbf{k}}$ for the angle α, and $\mathbf{Trans}(\mathbf{l})$ denote the homogeneous translation matrix translating for the vector $\mathbf{l}$. For example,

$$ \mathbf{Rot}(\hat{\mathbf{z}}, \alpha) = \begin{bmatrix} \cos\alpha & -\sin\alpha & 0 & 0 \\ \sin\alpha & \cos\alpha & 0 & 0 \\ 0 & 0 & 1 & 0 \\ 0 & 0 & 0 & 1 \end{bmatrix}, \text{ and } \mathbf{Trans}\left(\begin{bmatrix} l_x \\ l_y \\ l_z \end{bmatrix} \right) = \begin{bmatrix} 1 & 0 & 0 & l_x \\ 0 & 1 & 0 & l_y \\ 0 & 0 & 1 & l_z \\ 0 & 0 & 0 & 1 \end{bmatrix}. \tag{2} $$

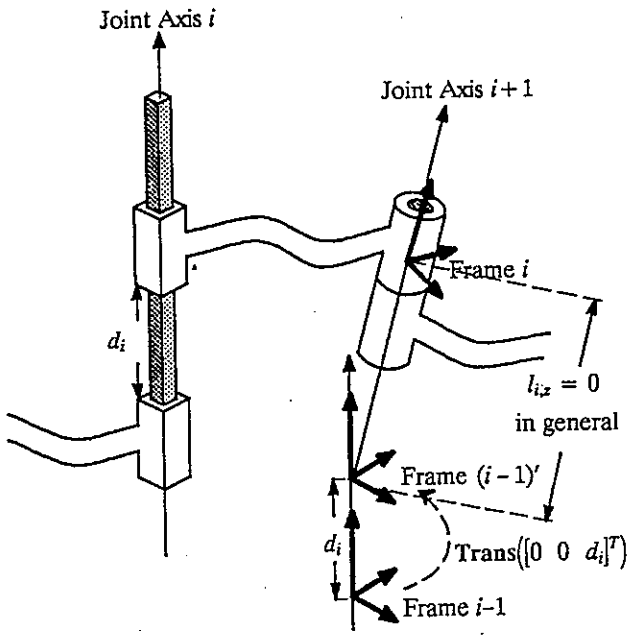

Fig. 3. CPC modeling convention
for a prismatic joint

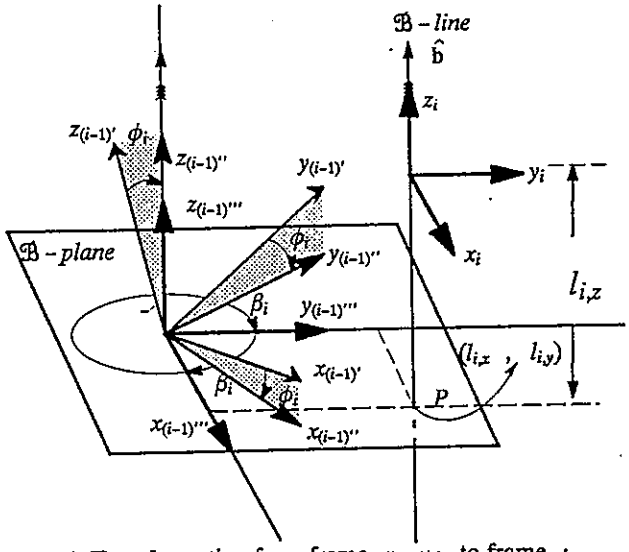

Fig. 4. Transformation from frame $(i-1)'$ to frame i

As shown in Fig. 2. and Fig. 3., the CPC kenimatic model of two consecutive joint frames i–1 and i can be divided into two parts: one that transforms frame $i-1$ into $(i-1)'$, i.e. ${}^{i-1}\mathbf{T}_{(i-1)'}$ where ${}^{i-1}\mathbf{T}_{(i-1)'}$ is $\mathbf{Rot}(\hat{z}, \theta_i)$ for a revolute joint (see Fig. 2.) and is $\mathbf{Trans}([0\ \ 0\ \ d_i]^T)$ for a prismatic joint (see Fig. 3.); and one that transforms frame $(i-1)'$ into frame i, i.e. ${}^{(i-1)'}\mathbf{T}_i$. Notice that both the

coordinate frames $(i-1)'$ and i are attached to the ith link, thus ${}^{(i-1)'}\mathbf{T}_i$ is a constant transformation matrix and it can be explicitly expressed as (refer to Fig. 4.)

$$ {}^{(i-1)'}\mathbf{T}_i = \mathbf{R}_i \ \mathbf{Rot}(\hat{z}_i, \ \beta_i) \ \mathbf{Trans}([l_{i,x} \ \ l_{i,y} \ \ l_{i,z}]^T), \tag{3} $$

which will be explained in the following. Let $[b_{i,x} \ b_{i,y} \ b_{i,z}]^T$ be the unit vector of z_i–axis (i.e. the $i+1$st joint axis) represented in frame $(i-1)'$.

(1) $\mathbf{R}_i$: As shown in Fig. 4., the rotation matrix $\mathbf{R}_i$ transforms frame $(i-1)'$ to frame $(i-1)''$ such that $z_{(i-1)''}$–axis is parallel to the $i+1$st joint axis. To specify the joint axis $i+1$, two parameters $b_{i,x}$ and $b_{i,y}$ are sufficient while $b_{i,z}$ can be computed from $\sqrt{1-b_{i,x}^2-b_{i,y}^2}$. Note that in the CPC model, the z–axes of any two consecutive joint frames should have positive inner product, since we have chosen $b_{i,z} \geq 0$. Let the unit vector $\hat{\mathbf{k}} \equiv \hat{z}_{(i-1)'} \times \hat{z}_i / \| \hat{z}_{(i-1)'} \times \hat{z}_i \|$, and the rotation angle $\phi \equiv \cos^{-1}(\hat{z}_{(i-1)'} \cdot \hat{z}_i)$, then we have (see Fig. 4., also refer to [23])

$$ \mathbf{R}_i \equiv \mathbf{Rot}(\hat{\mathbf{k}}, \phi) = \begin{bmatrix} 1-\dfrac{b_{i,x}^2}{1+b_{i,z}} & \dfrac{-b_{i,x}b_{i,y}}{1+b_{i,z}} & b_{i,x} & 0 \\ \dfrac{-b_{i,x}b_{i,y}}{1+b_{i,z}} & 1-\dfrac{b_{i,y}^2}{1+b_{i,z}} & b_{i,y} & 0 \\ -b_{i,x} & -b_{i,y} & b_{i,z} & 0 \\ 0 & 0 & 0 & 1 \end{bmatrix}. \tag{4} $$

(2) $\mathbf{Rot}(\hat{z}_i, \beta_i)$: Since we should not violate the CPC convention 1, the directions of x and y–axes can only be adjusted by rotating about the z –axis for the angle β_i to the desired orientation. This rotation can be expressed by $\mathbf{Rot}(\hat{z}_i, \beta_i)$. In general, the exact orientation of the x–axis of the joint frames, other than the end–effector and world coordinate frames, are not important. If there is no special specifications, e.g., a nominal model, the orientation of the x–axis of frame i can be assigned to be that of frame $(i-1)''$, then the rotation matrix $\mathbf{Rot}(\hat{z}_i, \beta_i)$ is not needed. That is β_i is zero by default,

unless a specific orientation of the x–axis of the joint frame i is required.

(3) **Trans**$([l_{i,x}\ l_{i,y}\ l_{i,z}]^T)$: The translation is performed by using the translating transformation matrix **Trans**$([l_{i,x}\ l_{i,y}\ l_{i,z}]^T)$. Here, we do not need all the three components $l_{i,x}$, $l_{i,y}$, and $l_{i,z}$ when sepcifying link transformation ${}^{(i-1)'}\mathbf{T}_i$. For a revolute joint i, if frame i is not required to be located at a specific position, we need only two components $l_{i,x}$ and $l_{i,y}$ to translate frame $(i-1)'''$ to frame i (see Fig. 4). For a prismatic joint we do not even need the translation vector at all, ie $\mathbf{l}_i = 0$, and frame $(i-1)'$ is chosen to have the same origin as frame i. To assign a coordinate frame on a revolute joint, it is better to locate the origin of the frame right on the joint axis, otherwise the rotation will not only change the orientation but also change the origin of the frame with respect to another coordinate system. When the both consecutive joints are revolute, it is sufficient to translate the origin of frame $i-1$ to joint axis $i+1$ with two components $l_{i,x}$ and $l_{i,y}$, where $(l_{i,x}, l_{i,y})$ are the point where the joint axis $i+1$ intersects the x–y plane of frame $(i-1)''$, see Fig. 4. With only the measurement of orientaion and position of the end–effector, we can not determine the origin of the link frame associated with a prismatic joint. Thus the origin of a prismatic joint frame is located on the joint axis of the nearest revolute joint next to it, unless a nominal model is available (see Fig. 3.).

In the case of a revolute joint, the matrix ${}^{i-1}\mathbf{T}_i$, $i = 1, 2, ..., n-1$, is a function of seven parameters $\{b_{i,x}\ b_{i,y}\ b_{i,z}\ l_{i,x}\ l_{i,y}, l_{i,z}\ \beta_i\}$ and one joint variable θ_i, while in the case of a prismatic joint, the joint variable is d_i and the parameters are the same. The assignment rules for link parameters and joint variables are as follows.

For the ith joint, the value of the joint variable θ_i (or d_i) of the ith joint is equal to the reading of rotation angle (or translation length) of the transducer. The sign of the joint variable is determined with that, if the increamental direction of the transducer agrees with the right hand law determined by $\hat{z}_{i-1}$, then the sign is equal to that of the transducer. For a prismatic joint, the sign is determined by checking if the incremental direction of transducer is corresponding to the positive direction of $\hat{z}_{i-1}$. If the ith joint is revolute and no nominal model is available, then only four parameters is needed, i.e.

$\{b_{i,x}\ b_{i,y}\ l_{i,x}\ l_{i,y}\}$, and $b_{i,z} = \sqrt{1 - b_{i,x}^2 - b_{i,y}^2}$, $l_{i,z} = 0$, $\beta_i = 0$. If the ith joint is prismatic and also no nominal is available, the origin of the frame $(i-1)'$ coordinate system is defined to be the same as the origin of frame i, which is on the next revolute joint axis. That is, $l_{i,x}$ and $l_{i,y}$ are set to zero (refer to Fig. 3.). The parameters are $\{b_{i,x}\ b_{i,y}\}$, and $b_{i,z} = \sqrt{1 - b_{i,x}^2 - b_{i,y}^2}$, $l_{i,x} = l_{i,y} = l_{i,z} = 0$, $\beta_i = 0$.

To summarize the joint transformation ${}^{i-1}\mathbf{T}_i$ is given by

$$ {}^{i-1}\mathbf{T}_i = {}^{i-1}\mathbf{T}_{(i-1)'}\ {}^{(i-1)'}\mathbf{T}_i,\ i = 1, 2, ..., n. \tag{5} $$

where
$$ {}^{i-1}\mathbf{T}_{(i-1)'} = \begin{cases} \mathbf{Rot}(\hat{z}_{i-1}\ \theta_i), & \text{for a revolute joint.} \\ \mathbf{Trans}(0,\ 0,\ d_i), & \text{for a prismatic joint.} \end{cases} \tag{6} $$

and ${}^{(i-1)'}\mathbf{T}_i$ is shown in (3). The necessity of different CPC kinematic parameters for different links are shown in Table 1.

2.3 The CPC Kinematic Model for the IIS-Head

Table 1. Necessity of different CPC kinematic parameters for different links

Parameter	World to Base	Frame i–1 to Frame i				To End-Effector
		P – P	P – R	R – P	R – R	
b_x	N	N	N	N	N	N
b_y	N	N	N	N	N	N
b_z	R	R	R	R	R	R
β	N	R	R	R	R	N/R
l_x	N	R	R	N	N	N
l_y	N	R	R	N	N	N
l_z	N	R	R	R	R	N
DoF	6	2	2	4	4	6

N: Necessary, R: Redundent,
N/R: Necessity in general, redundent in our case
P – P: Prismatic to Prismatic, P – R: Prismatic to Revolute
R – P: Revolute to Prismatic, R – R: Revolute to Revolute
DoF: Degrees of Freedom.

Different coordinate frames associated with diffent joints of the IIS–Head are shown in Fig. 5.

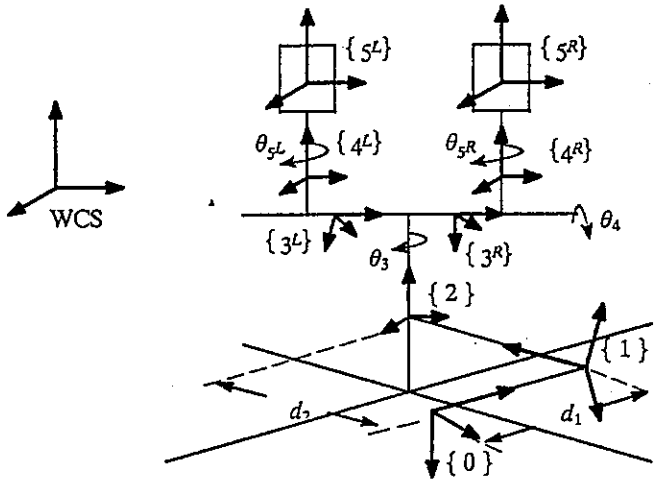

Fig. 5. Coordinate Frames and the skeleton diagram of the IIS–head.

The coordinate frames 5^L and 5^R are the end effector coordinate systems. By using the CPC kinematic model we have two transformation matrix ${}^{w}T_{5^L}$, ${}^{w}T_{5^R}$ which can be formulated as follows:

$$ {}^{w}T_{5^L} = {}^{w}T_0{}^{0}T_1{}^{1}T_2{}^{2}T_{3^L}{}^{3^L}T_{4^L}{}^{4^L}T_{5^L} \tag{7} $$

and

$$ {}^{w}T_{5^R} = {}^{w}T_0{}^{0}T_1{}^{1}T_2{}^{2}T_{3^R}{}^{3^R}T_{4^R}{}^{4^R}T_{5^R} \tag{8} $$

Since the calibration procedures, as will be described in section 4, are proceeded from the end–effector toward the base, frame i will be determined before frame i–1. Therefore, we will derive the kinematic model of the IIS–head from the end–effector to the base frame. As shown in Fig. 5., the last joints of both the left and right kinematic chains are revolute. In general, if we specify the joint frames from the base toward the end–effector, then we have already assigned the frames 4^L and 4^R. In this case the transformation to each end–effector frame have to use all the six degrees of freedom. But in the calibraion procedure , we first have frames 5^L and 5^R, and want to determine the frames 4^L and 4^R on the joint axes 5^L and 5^R, respectively. Here, we only need two degrees of freedom ($b_{i,x}$ $b_{i,y}$) provided by the CPC model for the rotation, but need all the three degrees of freedom

($l_{i,x}, l_{i,y}, l_{i,z}$) for the translation since the origin of the end–effector frame is specified. That is, we can omit β_{5^L} and β_{5^R} in equation (3) and obtain

$$ {}^{4^L}\mathbf{T}_{5^L} = \mathbf{Rot}(\hat{z}_4, \theta_5)\ \mathbf{R}_{5^L}\ \mathbf{Trans}\begin{bmatrix} l_{5^L x} \\ l_{5^L y} \\ l_{5^L z} \end{bmatrix}, \text{ and } \quad {}^{4^R}\mathbf{T}_{5^R} = \mathbf{Rot}(\hat{z}_4, \theta_5)\ \mathbf{R}_{5^R}\ \mathbf{Trans}\begin{bmatrix} l_{5^R x} \\ l_{5^R y} \\ l_{5^R z} \end{bmatrix}. \tag{9} $$

Transformations from frame 3^L and 3^R to 4^L and 4^R, respectively, are revolute joint to revolute joint frame transformations. As mentioned in section 2.2, we have

$$ {}^{3^L}\mathbf{T}_{4^L} = \mathbf{Rot}(\hat{z}_3, \theta_4)\ \mathbf{R}_{4^L}\ \mathbf{Trans}\begin{bmatrix} l_{4^L x} \\ l_{4^L y} \\ 0 \end{bmatrix}, \text{and} \quad {}^{3^R}\mathbf{T}_{4^R} = \mathbf{Rot}(\hat{z}_3, \theta_4)\ \mathbf{R}_{4^R}\ \mathbf{Trans}\begin{bmatrix} l_{4^R x} \\ l_{4^R y} \\ 0 \end{bmatrix}. \tag{10} $$

In Fig. 5. we can see that on the forth revolute joint, we have assigned two separate joint frames 3^L and 3^R. It may be confusing in the phase of kinematic modeling, but it would become clear in the parameter identification step. Notice that we have two end–effectors for the IIS–head. Starting from different end–effectors, we have different frames: 3^L and 3^R, which should be identical in the ideal case. But the CPC model only guarantees that both the z–axes of frame 3^L and 3^R are along the revolute joint 4. Let frame 3^L be the desired coordinate frame associated with joint axis 4. Then we have to rotate frame 3^R around the z–axis, which can be achieved by using the redundancy, β_3, as in following equation

$$ {}^{2}\mathbf{T}_{3^L} = \mathbf{Rot}(\hat{z}_2, \theta_3)\ \mathbf{R}_3\ \mathbf{Trans}\begin{bmatrix} l_{3^L x} \\ l_{3^L y} \\ 0 \end{bmatrix}, \text{and} \quad {}^{2}\mathbf{T}_{3^R} = \mathbf{Rot}(\hat{z}_2, \theta_3)\ \mathbf{R}_3\ \mathbf{Rot}(\hat{z}_3, \beta_3)\ \mathbf{Trans}\begin{bmatrix} l_{3^R x} \\ l_{3^R y} \\ 0 \end{bmatrix} \tag{11} $$

The first two joints are prismatic. Since we do not have the nominal model of the IIS–head, according to the explanation in section 2.2, we have

$$ {}^{1}\mathbf{T}_{2} = \mathbf{Trans}\begin{bmatrix} 0 \\ 0 \\ d_2 \end{bmatrix}\ \mathbf{R}_2\ \mathbf{Trans}\begin{bmatrix} 0 \\ 0 \\ 0 \end{bmatrix}, \tag{12} $$

and

$$ {}^{0}\mathbf{T}_{1} = \mathbf{Trans}\begin{bmatrix} 0 \\ 0 \\ d_1 \end{bmatrix}\ \mathbf{R}_1\ \mathbf{Trans}\begin{bmatrix} 0 \\ 0 \\ 0 \end{bmatrix}. \tag{13} $$

In general, the base frame (frame *0*) and the world frames (frame *w*) are specified somewhere on the robot base and in the working space, respectively. For the transformation from frame *w* to frame *0*, ${}^{w}\mathbf{T}_0$, all the six degrees of freedom in the CPC model have to be used, which yields

$$ {}^{w}\mathbf{T}_0 = \mathbf{R}_0\ \mathbf{Rot}(\hat{\mathbf{z}}_0, \beta_0)\ \mathbf{Trans}\begin{bmatrix} l_{0,x} \\ l_{0,y} \\ l_{0,z} \end{bmatrix}. \tag{14} $$

From equations (9)–(14), we have the following kinematic CPC model for the IIS–head :

$$ \left.\begin{matrix} {}^{w}\mathbf{T}_{5^L} \\ {}^{w}\mathbf{T}_{5^R} \end{matrix}\right\} = {}^{w}\mathbf{T}_0\ {}^{0}T_1\ {}^{1}\mathbf{T}_2\ \ \mathbf{Rot}(\hat{\mathbf{z}}_2, \theta_3)\ \ \mathbf{R}_3 \left\{\begin{matrix} \mathbf{Trans}\begin{bmatrix} l_{3^L,x} \\ l_{3^L,y} \\ 0 \end{bmatrix} \quad {}^{3^L}\mathbf{T}_{4^L}\ {}^{4^L}\mathbf{T}_{5^L} \\ \mathbf{Rot}(\hat{\mathbf{z}}_3, \beta_3)\ \mathbf{Trans}\begin{bmatrix} l_{3^R,x} \\ l_{3^R,y} \\ 0 \end{bmatrix}\ {}^{3^R}\mathbf{T}_{4^R}\ {}^{4^R}\mathbf{T}_{5^R} \end{matrix}\right. \tag{15} $$

3. DATA COLLECTION WITH A STEREO VISION SYSTEM

3.1 Techniques for Data Collection

From the user point of view the calibration measurement technique should meet certain requirements imposed by the application. Ideally, calibration should be automatic, non–invasive, fast, reliable and of low cost. A number of different approaches have been used for the measurement step in robot calibration. The two most popular ways to acquire the position and orientation data of the end–effector are the one using theodolites[5][7][10][22] and the one using vision sensors [3][12][13][17][20]. In practice, the former requires manual measurement so it is rather laborious and not automatic. Also, its accuracy depends on operator's training and carefulness, so it may not be reliable. We choose to use stereo vision because the calibration process can be made automatic by using specially designed calibration setups and image processing techniques.

To get 3D measurements using stereo vision techniques it is inevitable to calibrate the cameras first. Camera calibration is the process of determining the internal geometric and optical characteristics of the camera (e.g., intrinsic parameters such as focal length, lens distortion, etc) and the 3D position and orientation of camera frame relative to a certain world coordinate system (extrinsic parame-

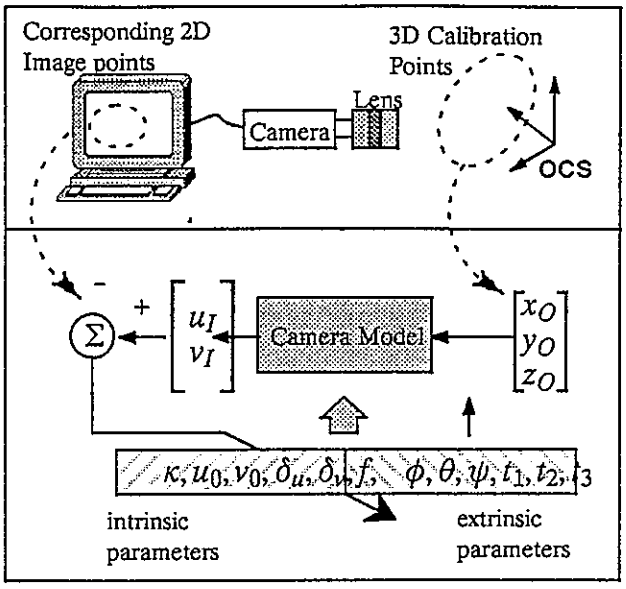

Fig. 6. Schematic diagram of camera calibration

ters). The schematic diagram of camera calibration is shown in Fig. 6. For details of camera calibration, refer to Shih[16] and Tsai[19].

For an eye–on–hand robot, if the origin of the end–effector coordinate system is defined to be on the lens center of the camera and if the calibration object can be kept within the viewfield during the measurement process, it is possible to estimate simultaneously the hand/eye and robot kinematic parameters together using the CPC model. However, when calibrating the IIS–head, it is difficult to always keep the calibration object within the viewfield while moving the joints of the head. Because of this difficulty, the method proposed by Lenz[12] is not applicable since their method requires that the calibration object remains within the viewfield when moving the robot.

3.2 Two Stage Procedure

To solve the above problem, we propose a two–stage procedure for calibrating the binocular head. In the first stage, the two cameras on the IIS–head are replaced by two small end–effector calibration plates having nine circles (see Fig. 7.). In this paper, the end effector, the camera mount, and the end–effector calibration plate coordinate systems are set to be identical, and defined to be the one attached to the nine–circle calibration plate shown in Fig. 7.. We define the origin of the end–effector coordinate system to be on the centroid of the central circle. The stereo cameras for measuring

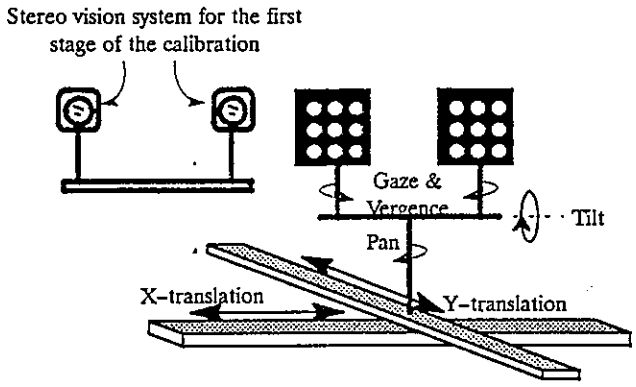

Fig. 7. The schematic diagram of the setup for the first stage of the calibration process

the orientations and positions of the calibration plates are set up such that both cameras can see the two plates under the planned head motion during calibration. The positions and orientations of the calibration plates, or equivalently, of the end–effectors, or of camera mounts, can be estimated using this stereo vision measurement system. Since the stereo vision measurement system is away from the binocular head and the calibration plates are mounted on the head, it is much easier to keep the calibration plates in the field of view while moving the joints of the head. The acquired positions and orientations of the calibration plates are then used to calibrate the kinematic parameters (section 4). In the second stage, the cameras are remounted to the IIS–head. We then use the method proposed by TsaiNO TAG to calibrate the hand–eye relation (section 5). Finally, the robot kinematic and the hand/eye relation are combined to provide a complete kinematic model for motion control.

3.3 Estimation of the Coordinate Transformation Matrix

Let $\{\mathbf{p}_i\}$ be the set of 3D positions of N circles in world coordinate system, measured by the stereo vision system, and $\{\mathbf{q}_i\}$ be their corresponding point set in the end–effector calibration plate coordinate system (i.e., frame 5^L or 5^R) . Note that $\{\mathbf{q}_i\}$ are known from the manufacture of the end–effector calibratoin plate. For example, $\mathbf{q}_i = (0\ 0\ 0)^T$ for the central point. Then for each 3D correspondence $\{\mathbf{p}_i, \mathbf{q}_i\}$, we have

$$\mathbf{q}_i = R\mathbf{p}_i + \mathbf{t} + \epsilon_i, \tag{16}$$

where R is the unknown 3 by 3 rotation matrix, $\mathbf{t}$ is the unknown 3 by 1 translation vector and ϵ_i is 3 by 1 noise vector. Define the error function as

$$E(R,\mathbf{t}) = \sum_{i=1}^{N} \| \mathbf{q}_i - (R\mathbf{p}_i + \mathbf{t}) \|^2 . \tag{17}$$

By setting $\nabla_t E(R,\mathbf{t}) = 0$, we have

$$\mathbf{t} = \overline{\mathbf{q}} - R\overline{\mathbf{p}}, \tag{18}$$

where $$\overline{\mathbf{p}} = \frac{1}{N}\sum_{i=1}^{N} \mathbf{p}_i \text{ and } \overline{\mathbf{q}} = \frac{1}{N}\sum_{i=1}^{N} \mathbf{q}_i .$$

Substituting (17) into (18), we have

$$E(R) = \sum_{i=1}^{N} \| \tilde{\mathbf{q}}_i - R\tilde{\mathbf{p}}_i \|^2, \tag{19}$$

where $$\tilde{\mathbf{p}}_i \equiv \mathbf{p}_i - \overline{\mathbf{p}} \text{ and } \tilde{\mathbf{q}}_i \equiv \mathbf{q}_i - \overline{\mathbf{q}} .$$

Rewrite equation (19) as

$$E(R) = \sum_{i=1}^{N} \| \tilde{\mathbf{q}}_i - (R\tilde{\mathbf{p}}_i) \|^2 = \sum_{i=1}^{N} \left[\tilde{\mathbf{q}}_i^T \tilde{\mathbf{q}}_i - 2\tilde{\mathbf{q}}_i^T R\tilde{\mathbf{p}}_i + \tilde{\mathbf{p}}_i^T \tilde{\mathbf{p}}_i \right] = \sum_{i=1}^{N} \left[\tilde{\mathbf{q}}_i^T \tilde{\mathbf{q}}_i + \tilde{\mathbf{p}}_i^T \tilde{\mathbf{p}}_i \right] - 2\sum_{i=1}^{N} \tilde{\mathbf{q}}_i^T R\tilde{\mathbf{p}}_i . \tag{20}$$

From (20), it can be shown that minimizing $E(R)$ is equivalent to maximize

$$\sum_{i=1}^{N} \tilde{\mathbf{q}}_i^T R\, \tilde{\mathbf{p}}_i = \sum_{i=1}^{N} trace[\tilde{\mathbf{q}}_i^T R\, \tilde{\mathbf{p}}_i] = \sum_{i=1}^{N} trace[R\, \tilde{\mathbf{p}}_i\, \tilde{\mathbf{q}}_i^T] = trace\left[R \sum_{i=1}^{N} \tilde{\mathbf{p}}_i\, \tilde{\mathbf{q}}_i^T \right]. \tag{21}$$

Thus, to minimize $E(R)$, it is essential to maximize $trace[R\ H]$, where

$$H \equiv \sum_{i=1}^{N} \tilde{\mathbf{p}}_i\, \tilde{\mathbf{q}}_i^T . \tag{22}$$

To solve for R which minimizes $E(R)$, we use the method proposed by Arun[2]. Performing the singular value decomposition of H, we have $H = USV^T$ where U and V are 3 by 3 orthonomal ma-

trices, and S is a 3 by 3 nonnegative diagonal matrix. Let $X \equiv VU^T$. Thus X is also an orthonormal matrix. If $\det(X) = +1$, then $R = X$ and $\mathbf{t} = \bar{\mathbf{q}} - R\bar{\mathbf{p}}$ is the optimal solution that minimizes (17).

4. KINEMATIC PARAMETERS IDENTIFICATION

Two kinds of techniques can be used to identify the kinematic parameters. The first one is an iterative method while the second one provides the closed–form solution to the kinematic parameters. For techniques that are of the first kind, the identification method is described as following. Let $\mathbf{p}(\mathbf{q}_k; \kappa)$ denote the end–effector–configuration vector, contains the position and/or orientation information of the end–effector, where $\mathbf{q}_k$ and κ denote the joint variables and kinematic parameters, respectively. Suppose we have made observations of the end–effector–configuration vector which are denoted as $\tilde{\mathbf{p}}_k$'s. Then the value of κ can be obtained by minimizing the error:

$$\mathbf{e}(\kappa) \equiv \sum_k \left\| \tilde{\mathbf{p}}_k - \mathbf{p}(\mathbf{q}_k; \kappa) \right\|^2 \tag{23}$$

As $\mathbf{e}(\cdot)$ is a nonlinear function of the kinematic parameters κ, this is a nonlinear optimization problem. Using first order Taylor expansion of the error, approximate linear differential models can be used[6][8][11][15]. In this paper, we use the second kind of techniques which provide closed form solutions[24]. Details are described as follows.

4.1 Problem Formulation for the Closed Form Solution

Let $\mathbf{q} \equiv [q_1, q_2, q_3, q_4, q_{5L}, q_{5R}]$, where q_i is the ith joint variable, $q_i \in \{\theta_i, d_i\}$. As defined in section 2, ${}^i\mathbf{T}_j$ is a homogeneous transformation relating link frame i and link frame j. Let ${}^i\mathbf{p}_j$ denote the translation vector of ${}^i\mathbf{T}_j$, and let ${}^iR_j$ be the upper–left 3×3 sub–matrix of ${}^i\mathbf{T}_j$. Denote the 3×1 column vectors of ${}^iR_j$ by ${}^i\mathbf{r}_{j,x}$, ${}^i\mathbf{r}_{j,y}$ and ${}^i\mathbf{r}_{j,z}$, that is ${}^iR_j \equiv \left[{}^i\mathbf{r}_{j,x} \;\; {}^i\mathbf{r}_{j,y} \;\; {}^i\mathbf{r}_{j,z}\right]$. Let $Rot(\hat{z}, \theta_i)$ and R_i denote the upper–left 3×3 sub–matrices of $\mathbf{Rot}(\hat{\mathbf{z}}, \theta_i)$ and $\mathbf{R}_i$, respectively. That is,

$$Rot(\hat{z}, \theta_i) = \begin{bmatrix} \cos\theta_i & -\sin\theta_i & 0 \\ \sin\theta_i & \cos\theta_i & 0 \\ 0 & 0 & 1 \end{bmatrix}. \tag{24}$$

Recall equation (4), each R_i is actually a matrix function of $b_{i,x}$ and $b_{i,y}$. Dividing equation (15), the CPC kinematic model for the IIS–head, into rotation matrix part and translation vector part, we have

$$ {}^{w}R_{5^L}(\mathbf{q}) = {}^{w}R_0\ R_1\ R_2\ Rot(\hat{\mathbf{z}}, q_3)\ R_3\ Rot(\hat{\mathbf{z}}, q_{4^L})\ R_{4^L}\ Rot(\hat{\mathbf{z}}, q_{5^L})\ R_{5^L}, \tag{25} $$

$$ {}^{w}R_{5^R}(\mathbf{q}) = {}^{w}R_0\ R_1\ R_2\ Rot(\hat{\mathbf{z}}, q_3)\ R_3\ Rot(\hat{\mathbf{z}}, \beta_3)\ Rot(\hat{\mathbf{z}}, q_{4^R})\ R_{4^R}\ Rot(\hat{\mathbf{z}}, q_{5^R})\ R_{5^R}, \tag{26} $$

$$ {}^{w}\mathbf{p}_{5^L}(\mathbf{q}) = {}^{w}R_0\ \mathbf{l}_0 + q_1\ {}^{w}\mathbf{r}_{0,z} + q_2\ {}^{w}\mathbf{r}_{1,z} + {}^{w}R_{3^L}(\mathbf{q})\ \mathbf{l}_{3^L} + {}^{w}R_{4^L}(\mathbf{q})\ \mathbf{l}_{4^L} + {}^{w}R_{5^L}(\mathbf{q})\ \mathbf{l}_{5^L}, \tag{27} $$

$$ {}^{w}\mathbf{p}_{5^R}(\mathbf{q}) = {}^{w}R_0\ \mathbf{l}_0 + q_1\ {}^{w}\mathbf{r}_{0,z} + q_2\ {}^{w}\mathbf{r}_{1,z} + {}^{w}R_{3^R}(\mathbf{q})\ \mathbf{l}_{3^R} + {}^{w}R_{4^R}(\mathbf{q})\ \mathbf{l}_{4^R} + {}^{w}R_{5^R}(\mathbf{q})\ \mathbf{l}_{5^R}, \tag{28} $$

where ${}^{w}R_0 = R_0\ Rot(\hat{\mathbf{z}}, \beta_0)$, ${}^{w}R_1 = {}^{w}R_0\ R_1$, ${}^{w}R_2 = {}^{w}R_1\ R_2$, ${}^{w}R_{3^L}(\mathbf{q}) = {}^{w}R_2\ Rot(\hat{\mathbf{z}}, q_3)\ R_3$,

$${}^{w}R_{3^R}(\mathbf{q}) = {}^{w}R_2\ Rot(\hat{\mathbf{z}}, q_3)\ R_3\ Rot(\hat{\mathbf{z}}, \beta_3),\ {}^{w}R_{4^L}(\mathbf{q}) = {}^{w}R_{3^L}(\mathbf{q})\ Rot(\hat{\mathbf{z}}, q_{4^L})\ R_{4^L},$$

$${}^{w}R_{4^R}(\mathbf{q}) = {}^{w}R_{3^R}(\mathbf{q})\ Rot(\hat{\mathbf{z}}, q_{4^R})\ R_{4^R}.$$

In equations (25)–(28), the kinematic parameters to be estimated are $(b_{0,x}\ b_{0,y})$, $(b_{1,x}\ b_{1,y})$, $(b_{2,x}\ b_{2,y})$, $(b_{3,x}\ b_{3,y})$, $(b_{4^L,x}\ b_{4^L,y})$, $(b_{4^R,x}\ b_{4^R,y})$, $(b_{5^L,x}\ b_{5^L,y})$, $(b_{5^R,x}\ b_{5^R,y})$, β_0, β_3, $\mathbf{l}_0 \equiv [l_{0,x}\ l_{0,y}\ l_{0,z}]^T$, $\mathbf{l}_{3^L} \equiv [l_{3^L,x}\ l_{3^L,y}\ 0]^T$, $\mathbf{l}_{3^R} \equiv [l_{3^R,x}\ l_{3^R,y}\ 0]^T$, $\mathbf{l}_{4^L} \equiv [l_{4^L,x}\ l_{4^L,y}\ 0]^T$, $\mathbf{l}_{4^R} \equiv [l_{4^R,x}\ l_{4^R,y}\ 0]^T$, $\mathbf{l}_{5^L} \equiv [l_{5^L,x}\ l_{5^L,y}\ l_{5^L,z}]^T$ and $\mathbf{l}_{5^R} \equiv [l_{5^R,x}\ l_{5^R,y}\ l_{5^R,z}]^T$. Notice that joints 1 and 2 are prismatic, thus according to the CPC model convention $\mathbf{l}_1$ and $\mathbf{l}_2$ are set to zero if there is no nominal model available.

When we move the IIS–head to a specific configuration, say $\mathbf{q}$, we can obtain the coordinate transformation matrix from WCS to the end–effecotr coordinate system, i.e. ${}^{5^L}\mathbf{T}_w(\mathbf{q})$ and ${}^{5^R}\mathbf{T}_w(\mathbf{q})$, using the stereo vision system as described in section 3.

In the following, the kinematic parameter identification problem will be reduced to that of finding a solution of linear algebraic equations. At least $N+1$ robot configuration measurements are needed for a complete identification for an N degrees of freedom robot. The measurement starts at an initial robot configuration which is denoted as $\mathbf{q}_0 = [q_{10},\ q_{20},\ q_{30},\ q_{40},\ q_{5^L0},\ q_{5^R0}]$. It proceeds by moving one joint at a time, as shown in Fig. 8.. For convenience, in the rest of this paper we will use $\mathbf{q}_{ik}$ to denote the configuration $[q_{10},\ q_{20},\ \ldots,\ q_{ik},\ \ldots,\ q_{5^L0},\ q_{5^R0}]$, which is identical to $\mathbf{q}_0$ except for the ith joint variable q_{i0} is replaced by q_{ik}. Thus, if one makes M measurements for each joint, then he will have $M \times N + 1$ transformation matrices with each associated with a specific configura-

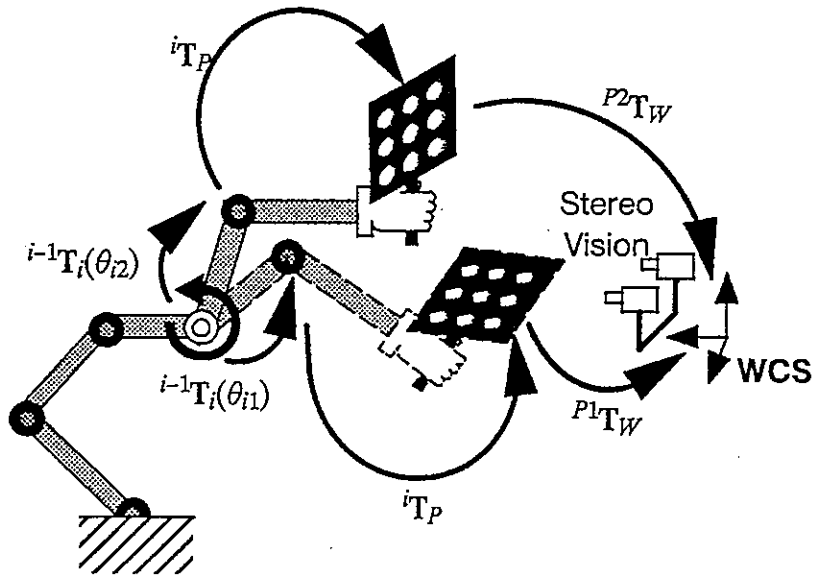

$$^{i-1}T_i(\theta_{i1})\,^{i}T_P\,^{P1}T_W = {}^{i-1}T_i(\theta_{i2})\,^{i}T_P\,^{P2}T_W \quad \Rightarrow \mathbf{A\,X = X\,B}$$

Fig. 8. Moving one joint at a time

tion $\mathbf{q}_{ik}$, i.e. $^{5L}T_w(\mathbf{q}_{ik})$ and $^{5R}T_w(\mathbf{q}_{ik})$, for $i = 1, 2, ..., N$ and $k = 0, 1, 2, ..., M$ (note that $\mathbf{q}_{i0}$ and $\mathbf{q}_0$ are identical).

4.2 Kinematic parameters identification of the IIS-head

In this section, we describe the closed-form solution for the IIS-head kinematic parameters identification problem. The computation can be divided into the following three steps.

Step 1. Determination of R_3, R_{4^L}, R_{4^R}, R_{5^L}, R_{5^R} *and* β_3

In this step, the matrices R_{5^L}, R_{5^R}, R_{4^L}, R_{4^R}, R_3, and $^{W}R_2$ are solved for (in this order) one by one. For example, R_3 is determined after both R_{5^L}, R_{5^R} and R_{4^L}, R_{4^R} are determined.

Step 1-a. Determination of R_{5^L} and R_{5^R}:

Since the calibration procedure for R_{5^L} and R_{5^R} are identical, we will omit the notation 'L' and 'R' that distinquishes them. The measurement process starts by moving the IIS-head to M positions, say $\mathbf{q}_{51}$, $\mathbf{q}_{52}$, ..., $\mathbf{q}_{5M}$ and then $^{5}T_w(\mathbf{q}_{5k})$, $k = 1, 2, ..., M$, are estimated by stereo measurement as explained in Section 3. Since all joints other than the fifth one are not moved, so the coordinate frame

transformation matrix from the forth joint frame to the WCS remains unchanged. Thus, for each configuration $\mathbf{q}_{5k}$ we have

$$ {}^4R_w(\mathbf{q}_{50}) = Rot(\hat{\mathbf{z}}, q_{50})\ R_5\ {}^5R_w(\mathbf{q}_{50}) = Rot(\hat{\mathbf{z}}, q_{5k})\ R_5\ {}^5R_w(\mathbf{q}_{5k}) = {}^4R_w(\mathbf{q}_{5k}) . \tag{29} $$

It then follows that

$$ Rot(\hat{\mathbf{z}}, q_{5k} - q_{50})\ R_5 = R_5\ {}^5R_w(\mathbf{q}_{50})\ {}^5R_w^{-1}(\mathbf{q}_{5k}) . \tag{30} $$

Taking transpose of equation (30), yields

$$ R_5^T\ Rot(\hat{\mathbf{z}}, q_{5k} - q_{50})^T = C_{5k}^T\ R_5^T , \tag{31} $$

where

$$ C_{5k} \equiv {}^5R_w(\mathbf{q}_{50})\ {}^5R_w^{-1}(\mathbf{q}_{5k}) . \tag{32} $$

Post multiplying equation (31) by $[0\ \ 0\ \ 1]^T$ and knowing that

$$ Rot(\hat{\mathbf{z}}, q_{5k} - q_{50})^T \begin{bmatrix} 0 \\ 0 \\ 1 \end{bmatrix} = \begin{bmatrix} 0 \\ 0 \\ 1 \end{bmatrix} , $$

we have

$$ C_i^T\ \mathbf{b}'_5 - \mathbf{b}'_5 = [C_i^T - \mathbf{I}]\ \mathbf{b}'_5 = 0 , \tag{33} $$

where

$$ \mathbf{b}'_5 \equiv \begin{bmatrix} -b_{5x} \\ -b_{5y} \\ b_{5z} \end{bmatrix} \text{ and } b_{5z} = \sqrt{1 - b_{5x}^2 - b_{5y}^2} . \tag{34} $$

Due to the observation noise, equation (33) may differ from zero for a small amount. Combining all the results from the M measurements we have

$$ \begin{bmatrix} C_{51}^T - \mathbf{I} \\ \vdots \\ C_{5M}^T - \mathbf{I} \end{bmatrix} \mathbf{b}'_5 \equiv \mathbf{C}_5\ \mathbf{b}'_5 = \epsilon \approx 0 \tag{35} $$

where ϵ is the error vector induced by the observation noise. The parameter vector $\mathbf{b}'_5$ can be estimated by minimizing $\| \epsilon \|^2$ subject to $\| \mathbf{b}'_5 \|^2 = 1$ and $b_{5z} \geq 0$. It can be shown that the solution to $\mathbf{b}'_5$ will be the eigenvector of $\mathbf{C}_5^T\mathbf{C}_5$ corresponding to the smallest eigenvalue.

Step 1–b. Determination of R_4 and R_4:

In order to estimate R_{4^L} and R_{4^R}, the procedures are similar to that used in the previous steps. Except that at this time the forth joints are moved while keeping other joints fixed, and the fifth joints have returned to their initial positions, i.e. $q_{5^L 0}$ and $q_{5^R 0}$. Similarly, the notation *'L'* and *'R'* are omitted and for each configuration $\mathbf{q}_{4i}$ we have

$$ {}^3R_w(\mathbf{q}_{40}) = Rot(\hat{\mathbf{z}}, q_{40})\ R_4\ {}^4R_5(\mathbf{q}_{40})\ {}^5R_w(\mathbf{q}_{40}) = Rot(\hat{\mathbf{z}}, q_{4k})\ R_4\ {}^4R_5(\mathbf{q}_{4k})\ {}^5R_w(\mathbf{q}_{4k}) = {}^3R_w(\mathbf{q}_{4k}) \quad (36) $$

Since the rotation matrix R_5 has been determined,

$$ {}^4R_5(\mathbf{q}_{4k}) = Rot(\hat{\mathbf{z}}, q_{50})\ R_5 \quad (37) $$

is now available. Also, ${}^5R_w(\mathbf{q}_{4k})$ is available from stereo measurement. Therefore, ${}^4R_w(\mathbf{q}_{4k}) = {}^4R_5(\mathbf{q}_{4k}){}^5R_w(\mathbf{q}_{4k})$ is also known. Using (36), we then have

$$ R_4^T\ Rot(\hat{\mathbf{z}}, q_{4k} - q_{40})^T = C_{4k}^T\ R_4^T, \quad (38) $$

where

$$ C_{4k} \equiv {}^4R_w(\mathbf{q}_{40})\ {}^4R_w^{-1}(\mathbf{q}_{4k}). \quad (39) $$

Similar to step 1–a, we have

$$ C_{4k}^T \mathbf{b}'_4 - \mathbf{b}'_4 = [C_{4k}^T - \mathbf{I}]\ \mathbf{b}'_4 = 0, \quad (40) $$

where

$$ \mathbf{b}'_4 \equiv \begin{bmatrix} -b_{4x} \\ -b_{4y} \\ b_{4z} \end{bmatrix} \text{ and } b_{4z} = \sqrt{1 - b_{4x}^2 - b_{4y}^2}. \quad (41) $$

The method for solving $\mathbf{b}'_4$ is identical to that depicted in step 1–a for solving $\mathbf{b}'_5$.

Step 1–c. Determination of β_3 :

By holding the first three joints fixed, i.e. ${}^wR_3(\mathbf{q})$ is fixed, from equations (25) and (26), we have

$$ {}^{4^L}R_w(\mathbf{q}) = Rot(\hat{\mathbf{z}}, \beta_3)\ {}^{4^R}R_w(\mathbf{q}), \quad (42) $$

where

$$ {}^{4^L}R_w(\mathbf{q}) = Rot(\hat{\mathbf{z}}, q_4)\ R_{4^L}\ Rot(\hat{\mathbf{z}}, q_{5^L})\ R_{5^L}\ {}^{5^L}R_w(\mathbf{q}), $$

and

$$ {}^{4^R}R_w(\mathbf{q}) = Rot(\hat{\mathbf{z}}, q_4)\ R_{4^R}\ Rot(\hat{\mathbf{z}}, q_{5^R})\ R_{5^R}\ {}^{5^R}R_w(\mathbf{q}). \quad (43) $$

Note that ${}^{4^L}R_w(\mathbf{q}_{ik})$ and ${}^{4^R}R_w(\mathbf{q}_{ik})$ $i = 4,\ 5^L$ and 5^R, $k = 0, 1, ..., M$, are all known since ${}^{5^L}R_w(\mathbf{q}_{ik})$ and ${}^{5^R}R_w(\mathbf{q}_{ik})$ are available from stereo measurements, R_{5^L}, R_{5^R}, R_{4^L}, R_{4^R} are determined from steps 1–a and 1–b, and $Rot(\hat{\mathbf{z}}, q_{ik})$ can be computed easily given q_{ik}. Rewrite equation (42) as follows,

$$\begin{bmatrix} a_{ik1} & a_{ik2} & a_{ik3} \\ a_{ik4} & a_{ik5} & a_{ik6} \\ a_{ik7} & a_{ik8} & a_{ik9} \end{bmatrix} = \begin{bmatrix} \cos\beta_3 & -\sin\beta_3 & 0 \\ \sin\beta_3 & \cos\beta_3 & 0 \\ 0 & 0 & 1 \end{bmatrix} \begin{bmatrix} b_{ik1} & b_{ik2} & b_{ik3} \\ b_{ik4} & b_{ik5} & b_{ik6} \\ b_{ik7} & b_{ik8} & b_{ik9} \end{bmatrix}, \tag{44}$$

where $\begin{bmatrix} a_{ik1} & a_{ik2} & a_{ik3} \\ a_{ik4} & a_{ik5} & a_{ik6} \\ a_{ik7} & a_{ik8} & a_{ik9} \end{bmatrix} \equiv {}^{4^L}R_w(\mathbf{q}_{ik})$, and $\begin{bmatrix} b_{ik1} & b_{ik2} & b_{ik3} \\ b_{ik4} & b_{ik5} & b_{ik6} \\ b_{ik7} & b_{ik8} & b_{ik9} \end{bmatrix} \equiv {}^{4^L}R_w(\mathbf{q}_{ik})$.

Therefor, we have

$$\begin{bmatrix} b_{ik1} & -b_{ik4} \\ b_{ik2} & -b_{ik5} \\ b_{ik3} & -b_{ik6} \\ b_{ik4} & b_{ik1} \\ b_{ik5} & b_{ik2} \\ b_{ik6} & b_{ik3} \end{bmatrix} \begin{bmatrix} \cos\beta_3 \\ \sin\beta_3 \end{bmatrix} = \begin{bmatrix} a_{ik1} \\ a_{ik2} \\ a_{ik3} \\ a_{ik4} \\ a_{ik5} \\ a_{ik6} \end{bmatrix}. \tag{45}$$

For all the configurations, $\mathbf{q}_{ik}$, $i = 4,\ 5^L$ and 5^R, $k = 0, 1, ..., M$, construct an overdetermined system and solve for the two unknowns, $\cos\beta_3$ and $\sin\beta_3$, subject to $\sin^2\beta_3 + \cos^2\beta_3 = 1$. Then β_3 can be obtained from $\cos\beta_3$ and $\sin\beta_3$.

Step 1–d. Determination of R_3:

To estimate R_3, all the joints are moved to their initial positions, $\mathbf{q}_0$, then the stereo measurements of the end–effector calibration plate are performed for the configurations where only joint three are moved, $\mathbf{q}_{3k}$, $k = 1, 2, ..., M$. Unlike the previous calibration procedures, the kinematic chains are now combined in joint three. Thus the informations from two kinematic chains can be used together to calibrate R_3. Since the transformation matrix from joint frame two to the WCS are not changed, when only joint three is moved, we have

$$ {}^2R_w(\mathbf{q}_{30}) = Rot(\hat{\mathbf{z}}, q_{30}) R_3 {}^{3^L}R_{5^L}(\mathbf{q}_{30}) {}^{5^L}R_w(\mathbf{q}_{30}) = Rot(\hat{\mathbf{z}}, q_{3k}) R_3 {}^{3^L}R_{5^L}(\mathbf{q}_{3k}) {}^{5^L}R_w(\mathbf{q}_{3k}) = {}^2R_w(\mathbf{q}_{3k}) \,, \quad (46) $$

and
$$ {}^2R_w(\mathbf{q}_{30}) = Rot(\hat{\mathbf{z}}, q_{30})\ R_3\ Rot(\hat{\mathbf{z}}, \beta_3)\ {}^{3^R}R_{5^R}(\mathbf{q}_{30})\ {}^{5^R}R_w(\mathbf{q}_{30}) $$
$$ = Rot(\hat{\mathbf{z}}, q_{3k})\ R_3\ Rot(\hat{\mathbf{z}}, \beta_3)\ {}^{3^R}R_{5^R}(\mathbf{q}_{3k})\ {}^{5^R}R_w(\mathbf{q}_{3k}) = {}^2R_w(\mathbf{q}_{3k}) \,, \quad (47) $$

where
$$ {}^{3^L}R_{5^L}(\mathbf{q}_{3k}) = Rot(\hat{\mathbf{z}}, q_{40}) R_{4^L} Rot(\hat{\mathbf{z}}, q_{5^L 0}) R_{5^L} $$

and
$$ {}^{3^R}R_{5^R}(\mathbf{q}_{3k}) = Rot(\hat{\mathbf{z}}, q_{40}) R_{4^R} Rot(\hat{\mathbf{z}}, q_{5^R 0}) R_{5^R} \,. $$

Let
$$ {}^{3^L}R_w(\mathbf{q}_{3k}) \equiv {}^{3^L}R_{5^L}(\mathbf{q}_{3k}) {}^{5^L}R_w(\mathbf{q}_{3k}) \text{ and } {}^{3^R}R_w(\mathbf{q}_{3k}) \equiv {}^{3^R}R_{5^R}(\mathbf{q}_{3k}) {}^{5^R}R_w(\mathbf{q}_{3k}) \,. \quad (48) $$

From equations (46) and (47), we have

$$ R_3^T\ Rot^T(\hat{\mathbf{z}}, q_{3k} - q_{30}) = C_{3k^L}^T\ R_3^T \,, \quad (49) $$

$$ R_3^T\ Rot^T(\hat{\mathbf{z}}, q_{3k} - q_{30}) = C_{3k^R}^T\ R_3^T \,, \quad (50) $$

where $C_{3k^L} \equiv {}^{3^L}R_w(\mathbf{q}_{30}) {}^{3^L}R_w^{-1}(\mathbf{q}_{3k})$ and $C_{3k^R} \equiv Rot(\hat{\mathbf{z}}, \beta_3)\ {}^{3^R}R_w(\mathbf{q}_{30}) {}^{3^R}R_w^{-1}(\mathbf{q}_{3k})\ Rot^{-1}(\hat{\mathbf{z}}, \beta_3)$. (51)

Similar to the previous steps, we have
$$ \begin{bmatrix} C_{3k^L}^T - \mathbf{I} \\ C_{3k^R}^T - \mathbf{I} \end{bmatrix} \mathbf{b}'_3 = 0 \,, \quad (52) $$

where
$$ \mathbf{b}'_3 \equiv \begin{bmatrix} -b_{3x} \\ -b_{3y} \\ b_{3z} \end{bmatrix} \text{ and } b_{3z} = \sqrt{1 - b_{3x}^2 - b_{3y}^2} \,. \quad (53) $$

Step 1–e. Determination of ${}^wR_2$:

After R_{5^L}, R_{4^L}, and R_3 are obtained, we can compute ${}^2R_{5^L}$ from the following

$$ {}^2R_{5^L}(\mathbf{q}) = Rot(\hat{\mathbf{z}}, q_3)\ R_3\ Rot(\hat{\mathbf{z}}, q_4)\ R_{4^L}\ Rot(\hat{\mathbf{z}}, q_{5^L})\ R_{5^L} \,, \quad (54) $$

which yields

$$ {}^wR_2 = \left[{}^2R_{5^L}(\mathbf{q})\ {}^{5^L}R_w(\mathbf{q}) \right]^{-1} = {}^{5^L}R_w^T(\mathbf{q})\ {}^2R_{5^L}^T(\mathbf{q}) \,. \quad (55) $$

Alternatively, we can obtain ${}^wR_2$ from the other chain by computing ${}^2R_{5^R}$

$$ {}^2R_{5^R}(\mathbf{q}) = Rot(\hat{\mathbf{z}}, q_3)\ R_3\ Rot(\hat{\mathbf{z}}, \beta_3)\ Rot(\hat{\mathbf{z}}, q_4)\ R_{4^R}\ Rot(\hat{\mathbf{z}}, q_{5^R})\ R_{5^R} \,, \quad (56) $$

yields
$$ {}^wR_2 = \left[{}^2R_{5^R}(\mathbf{q})\ {}^{5^R}R_w(\mathbf{q}) \right]^{-1} = {}^{5^R}R_w^T(\mathbf{q})\ {}^2R_{5^R}^T(\mathbf{q}) \,. \quad (57) $$

Notice that since there is no revolute joint between the WCS and the second joint frame, so the transformation matrix ${}^{w}R_2$ is a constant matrix, i.e. it cannot be altered by changing the joint variables of d_1 and d_2.

Step 2. Determination of $\mathbf{l}_{3^L}$, $\mathbf{l}_{3^R}$, $\mathbf{l}_{4^L}$, $\mathbf{l}_{4^R}$, $\mathbf{l}_{5^L}$ *and* $\mathbf{l}_{5^R}$

Consider (27) and (28). Since ${}^{w}R_0$ and $\mathbf{l}_0$ are both unknown, the problem of solving $\mathbf{l}_0$ usgin (27) and (28) is a nonlinear problem. To simplify the problem, define $\mathbf{l}'_2$ such that $\mathbf{l}_0 = R_1\, R_2\, \mathbf{l}'_2$. Then (27) and (28) can be rewritten as

$$ {}^{w}\mathbf{p}_{5^L}(\mathbf{q}) = q_1\, {}^{w}\mathbf{r}_{0,z} + q_2\, {}^{w}\mathbf{r}_{1,z} + {}^{w}R_2\, \mathbf{l}'_2 + {}^{w}R_{3^L}(\mathbf{q})\, \mathbf{l}_{3^L} + {}^{w}R_{4^L}(\mathbf{q})\, \mathbf{l}_{4^L} + {}^{w}R_{5^L}(\mathbf{q})\, \mathbf{l}_{5^L}, \quad (58) $$

and $$ {}^{w}\mathbf{p}_{5^R}(\mathbf{q}) = q_1\, {}^{w}\mathbf{r}_{0,z} + q_2\, {}^{w}\mathbf{r}_{1,z} + {}^{w}R_2\, \mathbf{l}'_2 + {}^{w}R_{3^R}(\mathbf{q})\, \mathbf{l}_{3^R} + {}^{w}R_{4^R}(\mathbf{q})\, \mathbf{l}_{4^R} + {}^{w}R_{5^R}(\mathbf{q})\, \mathbf{l}_{5^R}, \quad (59) $$

Recall that we have set $\mathbf{l}_2 = 0$ in section 2.3. However, since we have the redundancy, $l_{2,z}$, instead of letting $l_{2,z} = 0$, we can select $l_{2,z}$ such that $\mathbf{l}'_2 + \mathbf{l}_2 = \left[l'_{2,x}\ l'_{2,y}\ 0\right]^T$. When choose the redundancy $l_{2,z}$ to eliminate $l'_{2,z}$, we are shifting the origin of the robot base frame.

Notice that, in Eqs (58) and (59), ${}^{w}\mathbf{p}_{5^L}$ and ${}^{w}\mathbf{p}_{5^R}$ are the positions of the origins of the left and right end-effector coordinate systems observed by the stereo measurement system in WCS; q_1 and q_2 are the prismatic joint values of joint 1 and 2. The rotation matrices, ${}^{w}R_2$, ${}^{w}R_{3^L}(\mathbf{q})$, ${}^{w}R_{3^R}(\mathbf{q})$, ${}^{w}R_{4^L}(\mathbf{q})$, ${}^{w}R_{4^R}(\mathbf{q})$, ${}^{w}R_{5^L}(\mathbf{q})$, ${}^{w}R_{5^R}(\mathbf{q})$, are obtained in the previous calibration step. The only unknowns left in equations (58) and (59) are

$$ \mathbf{x} \equiv \left[{}^{w}\mathbf{r}_{0,z}\ {}^{w}\mathbf{r}_{1,z}\ l'_{2,x}\ l'_{2,y}\ l_{3^L,x}\ l_{3^L,y}\ l_{4^L,x}\ l_{4^L,y}\ l_{5^L,x}\ l_{5^L,y}\ l_{5^L,z}\ l_{3^R,x}\ l_{3^R,y}\ l_{4^R,x}\ l_{4^R,y}\ l_{5^R,x}\ l_{5^R,y}\ l_{5^R,z}\right]^T. $$

(60)

Notice that equations (58) and (59) are linear in $\mathbf{x}$. For convinence, let ${}^{w}\tilde{R}_2$, ${}^{w}\tilde{R}_{3^L}(\mathbf{q})$, ${}^{w}\tilde{R}_{3^R}(\mathbf{q})$, ${}^{w}\tilde{R}_{4^L}(\mathbf{q})$ and ${}^{w}\tilde{R}_{4^R}(\mathbf{q})$ denote the first two columns of the rotation matrices ${}^{w}R_2$, ${}^{w}R_{3^L}(\mathbf{q})$, ${}^{w}R_{3^R}(\mathbf{q})$, ${}^{w}R_{4^L}(\mathbf{q})$ and ${}^{w}R_{4^R}(\mathbf{q})$, respectively.

For each configuration $\mathbf{q}_{ik}$, we have, from equation (58) and (59),

$$y(\mathbf{q}_{ik}) = G(\mathbf{q}_{ik})\ \mathbf{x} \tag{61}$$

where $G(\mathbf{q}_{ik}) = \begin{bmatrix} q_1\mathbf{I}_{3\times3} & q_2\mathbf{I}_{3\times3} & {}^{w}\bar{R}_2 & {}^{w}\bar{R}_{3^L}(\mathbf{q}_{ik}) & {}^{w}\bar{R}_{4^L}(\mathbf{q}_{ik}) & {}^{w}R_{5^L}(\mathbf{q}_{ik}) & 0_{3\times2} & 0_{3\times2} & 0_{3\times3} \\ q_1\mathbf{I}_{3\times3} & q_2\mathbf{I}_{3\times3} & {}^{w}\bar{R}_2 & 0_{3\times2} & 0_{3\times2} & 0_{3\times3} & {}^{w}\bar{R}_{3^R}(\mathbf{q}_{ik}) & {}^{w}\bar{R}_{4^R}(\mathbf{q}_{ik}) & {}^{w}R_{5^R}(\mathbf{q}_{ik}) \end{bmatrix}$

(62)

and $$y(\mathbf{q}_{ik}) = \begin{bmatrix} {}^{w}\mathbf{p}_{5^L}(\mathbf{q}_{ik}) \\ {}^{w}\mathbf{p}_{5^R}(\mathbf{q}_{ik}) \end{bmatrix}. \tag{63}$$

Combining all the results for the configurations, $\mathbf{q}_{ik}$, $i = 1, 2, 3, 4, 5^L, 5^R$; $k = 0, 1, ..., M$, we have the overdetermined system

$$\mathbf{y} = \begin{bmatrix} y(\mathbf{q}_0) \\ \vdots \\ y(\mathbf{q}_{ik}) \\ \vdots \\ y(\mathbf{q}_{5^RM}) \end{bmatrix} = \begin{bmatrix} G(\mathbf{q}_0) \\ \vdots \\ G(\mathbf{q}_{ik}) \\ \vdots \\ G(\mathbf{q}_{5^RM}) \end{bmatrix} \mathbf{x} = \mathbf{G}\ \mathbf{x}\,. \tag{64}$$

The unknown parameters are identified by minimizing the error function $\| \mathbf{y} - \mathbf{G}\mathbf{x} \|^2$ subject to $\| {}^{w}r_{0z} \|^2 = 1$ and $\| {}^{w}r_{1z} \|^2 = 1$.

Step 3. Determination of R_0, R_1, R_2, β_0 *and* $\mathbf{l}_0$

In this step, R_0, R_1, R_2, β_0 and $\mathbf{l}_0$ are solved by using the results obtained in steps 1 and 2. Notice that ${}^{w}\mathbf{r}_{0z}$ is the third column of ${}^{w}R_0$, which is equal to the third column of ${}^{w}R_0 = R_0\ Rot(\hat{z}, \beta_0)$. Since $Rot(\hat{z}, \beta_0)$ dose not affect the third column of R_0, ${}^{w}\mathbf{r}_{0z}$ is also the third column of R_0, ie. ${}^{w}\mathbf{r}_{0z} = \mathbf{r}_{0z} = [b_{0,x}\ b_{0,y}\ b_{0,z}]^T$. Since ${}^{w}\mathbf{r}_{0z}$ has been determined in step 2, R_0 can be obtained using (4). To solve for R_2 and R_1, notice that ${}^{w}R_2 = {}^{w}R_1R_2$ and ${}^{w}R_1 = {}^{w}R_0R_1$, or equivalently, $R_2^T = {}^{w}R_2^{Tw}R_1$ and $R_1^T = {}^{w}R_1^{Tw}R_0$. Therefore,

$$\mathbf{b'}_2 = {}^{w}R_2^T\ {}^{w}\mathbf{r}_{1z} \tag{65}$$

$$\mathbf{b'}_1 = {}^{w}R_1^T\ {}^{w}\mathbf{r}_{0z} \tag{66}$$

where $\mathbf{b}'_i$, the third column of R_i^T, is $[-b_{i,x}, -b_{i,y}, b_{i,z}]^T$, $i = 1$ or 2. By using ${}^w\mathbf{r}_{1z}$ obtained in step 2 and ${}^wR_2$ obtained in step 1, $\mathbf{b}'_2$ can be solved using (65). Then R_2 can be obtained from (4). Next, noticing that ${}^wR_1 = {}^wR_2R_2^T$, $\mathbf{b}'_1$ can be obtained from (66), which leads to R_1. Finally,

$$\mathbf{l}_0' \equiv R_1 R_2 (\mathbf{l}'_2 + \mathbf{l}_2) \tag{67}$$

where $\mathbf{l}'_2 + \mathbf{l}_2 = [\, l'_{2,x} \;\; l'_{2,y} \;\; 0]^T$ and $l'_{2,x}$, $l'_{2,y}$ have been determined in section step 2.

5. HAND/EYE CALIBRATION

In the second stage of the calibration, we remount the cameras to the IIS–head to find the hand–eye relationship. The schematic diagram of the setup for the second stage of the calibration process is shown in Fig. 9. A black calibration plate, with 25 white disks on it, is mounted on a translation stage where the Object Coordinate System (OCS) is defined and the coordinates of the 25 white disk centers are known with respect to the OCS. The hand refers to the camera mount (end–effector calibration plate) coordinate system used in the first stage and the eye refers to the camera coordinate system (CCS) located at the lens center. Since the kinematic parameters of the IIS–head have been identified, so given the joint variables, $\mathbf{q}_k \equiv [q_{1k}, \; q_{2k}, \; q_{3k}, \; q_{4k}, \; q_{5^Lk}, \; q_{5^Rk}]^T$, the coordinate transformation matrices from the base coordinate frame to the camera mount coordinate frame, i.e. ${}^0T_{5^L}(\mathbf{q}_k)$ and ${}^0T_{5^R}(\mathbf{q}_k)$, are known. Performing the camera extrinsic calibration, we have ${}^{C^L}T_O(\mathbf{q}_k)$

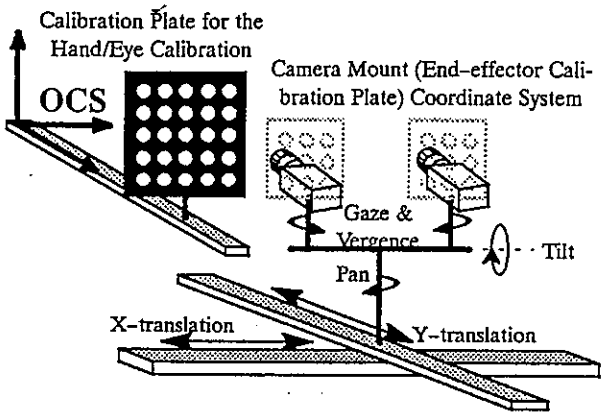

Fig. 9. The schematic diagram of the setup for the second stage of the calibration process

and ${}^{C^R}T_O(\mathbf{q}_k)$, the transformation matrices from the OCS to left and right CCS at the robot configuration $\mathbf{q}_k$. Thus the coordinate transformation matrix from the robot base frame to the OCS is

$$ {}^0T_O = {}^0T_{5^L}(\mathbf{q}_k)\ {}^{5^L}T_{C^L}\ {}^{C^L}T_O(\mathbf{q}_k) = {}^0T_{5^R}(\mathbf{q}_k)\ {}^{5^R}T_{C^R}\ {}^{C^R}T_O(\mathbf{q}_k)\,, \tag{68} $$

where the hand–eye relation ${}^{5^L}T_{C^L}$ and ${}^{5^R}T_{C^R}$ are unknowns to be estimated. Consider the left hand–eye relation first. For two different robot configurations $\mathbf{q}_k$ and $\mathbf{q}_j$, we have

$$ {}^0T_O = {}^0T_{5^L}(\mathbf{q}_k)\ {}^{5^L}T_{C^L}\ {}^{C^L}T_O(\mathbf{q}_k) = {}^0T_{5^L}(\mathbf{q}_j)\ {}^{5^L}T_{C^L}\ {}^{C^L}T_O(\mathbf{q}_j)\,. \tag{69} $$

Notice that, unlike the stage one calibration, since all the robot kinematic parameters are now available, it is not necessary to restrict the robot motion in such a way that only one joint can be moved at a time.

Rewrite (69) as

$$ A_{kj}\ {}^{5^L}T_{C^L} = {}^{5^L}T_{C^L}\ B_{kj}\,, \tag{70} $$

where

$$ A_{kj} \equiv {}^0T_{5^L}^{-1}(\mathbf{q}_j)\ {}^0T_{5^L}(\mathbf{q}_k) \text{ and } B_{kj} \equiv {}^{C^L}T_O(\mathbf{q}_j)\ {}^{C^L}T_O^{-1}(\mathbf{q}_k)\,, \tag{71} $$

where A_{kj} is obtained from the robot kinematic model and B_{kj} is obtained from the extrinsic camera calibration.

Let X denotes the unknown ${}^{5^L}T_{C^L}$, then equation (70) becomes of the form $AX = XB$. Many methods[21] can be used to solve for the algebraic equation, $AX = XB$, and we choose to use the technique proposed by Tsai[20] since accroding to Wang's experiments[21], Tsai's method has the smaller standard deviation than others.

To solve ${}^{5^L}T_{C^L}$ by Tsai's method, it is necessary to make measurements at least at three different robot configuratoins, say $\mathbf{q}_k$, $\mathbf{q}_j$ and $\mathbf{q}_i$, and during the robot motion at least two joints that are not parallel or anti–parallel have to be moved. In our case, the pan and tilt motions are adequate for the estimation of the hand–eye relation. The right hand–eye relation ${}^{5^R}T_{C^R}$ can also be obtained from a similar procedures.

6. EXPERIMENTS

Table 2. Specifications of IIS–head

Joint #	Type	Range	Resolution
1	Prismatic	0 – 1000 mm	0.005mm
2	Prismatic	0 – 500 mm	0.005mm
3	Revolute	0 – 180°	0.004°
4	Revolute	0 – 60°	0.005°
5^L	Revolute	0 – 90°	0.0036°
5^R	Revolute	0 – 90°	0.0036°

Table 3. DH kinematic parameters for IIS–head

Joint #	q	d	a	a
1	0°	q_1	–90°	0mm
2	90°	q_2	–90°	0mm
3	q_3	450mm	–90°	0mm
4	q_4	150mm	85°	50mm
5^L	q_5^L	100mm	0°	0mm
5^R	q_5^R	250mm	35°	70mm

To evaluate the accuracy of robot calibration, the positioning error is adopted as the error measure, where the positioning error is defined as the Euclidian distance between the measured and the CPC kinematic model positions of the end–effector. The specifications of the IIS–head are shown in Table 2. To collect measurement data, we have also setup a static stereo vision system, with the length of baseline equal to 600mm, which provides the accuracy of 0.5mm if the object distance is approximately 1.5 meter. In the simulation, we only add noise to measurement of the end–effector calibration plate, and do not add noise to the joint value, because the measurement error of the stereo vision system is much larger than the resolution of the joint variables. The kinematic parameters of the DH model of the IIS–head used in the simulation are contained in Table 3. In Table 3, the kinematic parameters are rough estimates of the true values, where θ is the rotation about axis z_{i-1} needed to make axis x_{i-1} parallel with axis x_i, d is the translation along z_{i-1} needed to make axis x_{i-1} intersect with axis x_i, a is the rotation about x_i needed to make axis z_{i-1} parallel with axis z_i, a is the translation along x_i needed to make axis z_{i-1} intersect with axsis z_i, refer to [4] for the details of DH model. Note that we have used the DH kinematic mode, since it is easier to be understood for the readers not

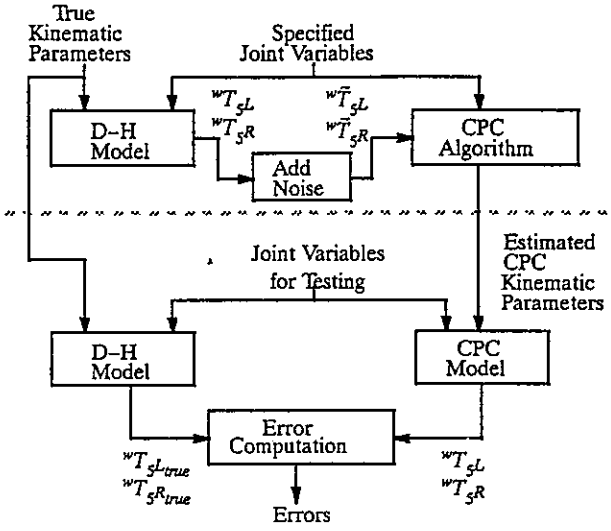

Fig. 10. Simulation process. ${}^{w}\mathbf{T}_{p}$ is the transformation matrix from plate coordinate system to world coordinate system.

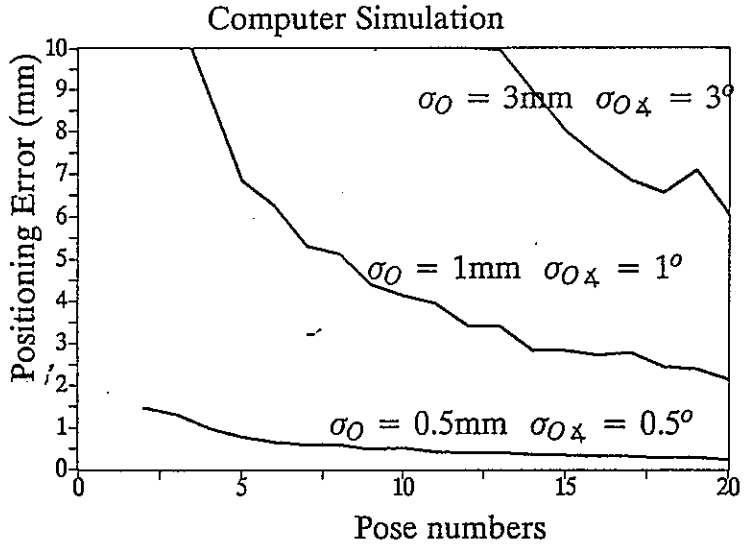

Fig. 11. The positioning error versus the measurement number and the standard deviation of the observation error.

familar with the CPC model. The schematic diagram for the computer simulations are shown in Fig. 10. The DH model generates a transformation matrix according to given joint values. The translation vector is then perturbed by adding noise with zero mean and standard deviation σ_O mm to its each entry. Rotation matrix is also perturbed by multiplying a rotation matrix with random rotation axis

Table 4. The calibration results from real experiments

Left Branch:		Right Branch:	
$\mu_x = 0.65mm$	$\sigma_x = 0.24mm$	$\mu_x = 0.28mm$	$\sigma_x = 0.31mm$
$\mu_y = 0.23mm$	$\sigma_y = 0.12mm$	$\mu_y = 0.13mm$	$\sigma_y = 0.21mm$
$\mu_z = 0.35mm$	$\sigma_z = 0.30mm$	$\mu_z = 0.11mm$	$\sigma_z = 0.35mm$

and random noise angle whose mean is zero and standard deviation is $\sigma_{O\&}$ degrees. The noisy transformation matrix is used as the measured one, and the calibration procedure described in section 4 are applied to the measured data and the joint variables. The estimated CPC kinematic parameters are then tested by computing the positioning error.

The first experiment is to determine the number of measurements has to be made for each joint. Fig. 11. shows the positioning errors of end–effector caused by robot calibration error. Each data point is the average of ten random trials. We find that for the requirement of 1mm calibration accuracy, the observation error should be controlled below 0.5mm and the number of measurement should be more than five, and we choose to use nine measurements for each joint.

In the real experiment, nine measurements are made for each joint as determined in the previous experiment. Currently, the hand–eye calibration is not completed yet. Thus only the calibration procedures described in section 4 are used to estimate the kinematic parameters. Due to the constraints that the calibration plates have to appear in the view field of the stereo cameras, the calibration ranges are smaller than the physical working ranges of the joint variables. Also, we have chosen nine poses of the IIS–head as the testing configuration set which are drawn from the calibration range (but the calibration procedures did not use this set). The mean and standard deviation of the positioning error in x, y and z directions are shown in Table 4, which shows that the positioning errors are less than 1mm in each direction.

7. CONCLUDING REMARKS

Many computer vision problems that are ill–posed, nonlinear or unstable for a passive observer become well–posed, linear or stable for an active observer[1]. Being able to acquire information actively, the active vision system has more potential applications than a passive one has. Specifically, in an active stereo vision system, the cameras are able to perform functions such as gazing, panning and tilting. To control the positions and orientations of the cameras, both the kinematic model and its

parameters of the active vision mechanism have to be known. Unfortunately, the exact kinematic parameters are usually unknown. In this paper we have solved the kinematic parameters identification problem for the IIS–head based on the CPC closed form solution[24]. Some modifications has to be made to the original CPC algorithm since the mechanism of an active binocular system has a branched kinematic chain having two branches, i.e., two chains sharing some common joints. We have extended the CPC method to handle this situation and still enjoy having closed form solution. The extended method can be directly used to solve the kinematic parameters for similar mechanism having branched chains. To control the active binocular system, we also have to develop an inverse kinematic solution for the CPC model with the estimated parameters. Our next goal is to develop an inverse kinematic solution, and implement the active vision paradigm on the IIS–head.

8. ACKNOWLEDGEMENTS

This research is supported in part by the National Science Council, Taiwan, ROC, under grant NSC 81–0408–E–001–04.

8. REFERENCES

[1]J. Aloimonos and A. Badyopadhyay, June 1987, "Active vision," in IEEE 1st Int. Conf. on Computer Vision, pp. 35–54.

[2]K.S. Arun, T.S. Huang, and S.D. Blostein, Sep. 1987, "Least–Squares Fitting of Two 3–D Point Sets," IEEE Trans. Pattern Anal. Machine Intell., vol. 9, no. 5, pp. 698–700.

[3]S. Chen, December 1987, "Robot Calibration using Stereo Vision," M.S. thesis, Florida Atlantic University.

[4]J. Denavit, R.S. Hartenberg, June 1955, "A Kinematic Notation for lower Pair Mechanisms Based on Matrices," ASME Journal of Applied Mechanics, pp. 215–221.

[5]M.R. Driels, U.S. Pathre, June 1991, "Vision–Based Automatic Theodolite for Robot Calibration," IEEE Transactions on Robotics and Automatics, vol. 7, NO. 3, pp. 351–360.

[6]G. Duelen, U. Kirchhoff, J. Held, 1988, "Methods of Identification of Geometrical Data in Robot Kinematics," Robotics & Computer–Integrated Manufacturing, Vol. 4, No. 1/2, pp. 181–185.

[7]G. Duelen, K. SchrÖer, 1991, "Robot Calibration–Method and Results," Robotics & Computer–Integrated Manufacturing, vol. 8, No. 4, pp. 223–231.

[8]L.J. Everett, A.H. Suryohadiprojo, 1988, "A Study of Kinematic Models for Forward Calibration of Manipulators," Proceedings of the International Conference on Robotics and Automation, pp. 798–800.

[9]Benjamin W. Mooring, Zvis Roth, Morris R. Driels, *Fundamental of Manipulator Calibration,* John Wiley & Sons. Inc. Publishers.

[10]R.P. Judd, A.B. Knasinski, Feb. 1990, "A Technique to Calibrate Industrial Robots with Experimental Verification," IEEE Transactions on Robotics and Automation, vol. 6, NO. 1, pp. 20–30.

[11]W. Khalil, M. Gautier, C. Enguehar, 1991, "Identifiable Parameters and Optimum Configurations for Robots Calibration," Robotica, vol. 9, pp. 63–70.

[12]R.K. Lenz, R.Y. Tsai, Sep. 1989, "Calibrating a Cartesian Robot with Eye–on–Hand Configuration Independent of Eye–to–Hand Relationship," IEEE Transactions on Pattern Analysis and Machine Intelligence, vol. 11, NO. 9, pp. 916–928.

[13]G.V. Puskorius, L.A. Feldkamp, 1987, "Global Calibration of a Robot/Vision System," Proceedings of the International Conference on Robotics and Automation, pp. 190–195.

[14]K.S. Roberts, 1988, "A New Representation for a Line," Proceedings of the International Conference on Computer Vision and Pattern Recognition, pp. 635–640.

[15]Z.S. Roth, B.W. Mooring, B.Ravani, Oct., 1987, "An Overview of Robot Calibration," IEEE Journal of Robotics and Automation, vol. RA–3, NO. 5, pp. 377–385.

[16]S.W. Shih, Y.P. Hung, W.S. Lin, November 1991, "A Fast and Accurate Camera Calibration Technique for 3D Computer Vision," Proceedings SPIE Conference on Optics, Illumination, and Image Sensing for Machine Vision VI, pp. 12–19.

[17]Y.C. Shiu, S.Ahmad, Feb. 1989, "Calibration of Wrist–Mounted Robotic Sensors by Solving Homogeneous Transform Equations of the Form AX = XB," IEEE Transactions on Robotics and Automation, vol. 5, NO. 1, pp. 16–29.

[18]H.W. Stone, 1987, *Kinematic Modeling, Identification, and Control of Robotic Manipulators*, kluwer Academic Publishers.

[19]R.Y. Tsai, 1987, "A Versatile Camera Calibration Technique for High–Accuracy 3D Machine Vision Metrology Using Off–the–Shelf TV Cameras and Lenses," IEEE Journal of Robotics and Automation, Vol. RA–3 No. 4, pp. 323–344.

[20]R.Y. Tsai, R.K. Lenz, June 1989, "A New Technique for Fully Autonomous and Efficient 3D Robotics Hand/Eye Calibration," IEEE Transactions on Robotics and Automation, vol. 5, NO. 3, pp. 345–358.

[21]C.C. Wang, April 1992, "Extrinsic Calibration of a Vision Sensor Mounted on a Robot," IEEE Journal of Robotics and Automation, vol. 8, no. 2, pp. 161–175.

[22]D.E. Whitney, C.A. Lozinski, March 1986, "Industrial Robot Forward Calibration Method and Results," Journal of Dynamic Systems, Measurement, and Control, vol. 108.

[23]H. Zhuang, Z.S. Roth, 1990, "A Complete and Parametrically Continuous Kinematic Model for Robot Manipulators," Proceedings of the International Conference on Robotics and Automation, pp. 92–97.

[24]H. Zhuang, Z.S. Roth, 1991, "A Closed Form Solution to the Kinematic Parameter Identification of Robot Manipulators," Proceedings of the International Conference on Robotics and Automation, pp. 2682–2688.